Pediatr Cardiol (2009) 30:626–634
DOI 10.1007/s00246-009-9406-5

RILEY SYMPOSIUM

Analysis of Ventricular Hypertrabeculation and Noncompaction Using Genetically Engineered Mouse Models

Hanying Chen · Wenjun Zhang · Deqiang Li · Tim M. Cordes · R. Mark Payne · Weinian Shou

Received: 5 February 2009 / Accepted: 26 February 2009 / Published online: 25 April 2009

Abstract Ventricular trabeculation and compaction are two of the many essential steps for generating a functionally competent ventricular wall. A significant reduction in trabeculation is usually associated with ventricular compact zone deficiencies (hypoplastic wall), which commonly lead to embryonic heart failure and early embryonic lethality. In contrast, hypertrabeculation and lack of ventricular wall compaction (noncompaction) are closely related defects in cardiac embryogenesis associated with left ventricular noncompaction, a genetically heterogeneous disorder. Here we summarize our recent findings through the analyses of several genetically engineered mouse models that have defects in cardiac trabeculation and compaction. Our data indicate that cellular growth and differentiation signaling pathways are keys in these ventricular morphogenetic events.

Keywords Ventricular development · Trabeculation and compaction · Signaling

During mammalian embryonic heart development, the ventricles undergo a series of morphogenetic developments [3, 28, 42]. Ventricular trabeculation and compaction are two of the many essential steps for generating a functionally competent ventricular wall [38]. Simplistically, development of the ventricular wall has four distinct stages. Stage 1 is the formation of a single-cell layered myocardium at an early developmental stage. Following induction via adjacent endoderm, lateral mesoderm gives rise to an early tubular heart. The heart at this stage is composed of a one-cell layer of myocardium and a one-cell layer of endocardium lining the lumen [3, 6]. Stage 2 is the formation of a trabeculated and compact myocardium at the early midgestation stage. As the myocardium thickens, cardiomyocytes along the inner wall form sheet-like protrusions into the lumen to give rise to the trabecular myocardium, while the outside layer of myocardium becomes organized into compact myocardium. Ventricular trabeculation has been suggested to facilitate oxygen and nutrient exchange and to enhance force generation to match the increasing blood flow in developing embryos [3, 38]. Stage 3, myocardial compaction, occurs at the late midgestation stage. As development proceeds, the trabecular myocardium becomes compacted toward the myocardial wall and contributes to forming a thicker, compact ventricular wall. The majority of trabeculae have become compacted after E14.5 in mouse embryos [33, 38]. Stage 4 is the formation of a mature and multilayered spiral myocardium during the late fetal and neonatal stage [26, 42].

Following the formation of primitive trabecular ridges (about E9.5 in mouse embryo; start of stage 2), the myocardium undergoes extensive expansion either by recruitment of cardiomyocytes from the myocardial wall into the trabecular ridges or via cellular proliferation within the trabecular cardiomyocytes. In support of the cellular recruitment mechanism, proliferative activity is consistently higher within the compact myocardium, as there is a gradient of decreasing proliferation and increased differentiation from the outside of the heart toward the lumen and trabecular side [16, 17, 31, 35]. This balance of proliferation and differentiation is critical to the formation of a functionally competent ventricular wall. Fate mapping

H. Chen · W. Zhang · D. Li · T. M. Cordes · R. Mark Payne · W. Shou (✉)
Riley Heart Research Center, Herman B. Wells Center for Pediatric Research, Department of Pediatrics, Indiana University School of Medicine, Indianapolis, IN 46202, USA
e-mail: wshou@iupui.edu

experiments using retroviral tagging with β-galactosidase in developing chick hearts have provided important insights into the interplay between cellular proliferation and ventricular wall formation [24, 25]. Upon myogenic differentiation, single labeled cardiomyocytes give rise to transmural and cone-shaped growth units. This pattern of growth is closely associated with the formation of the trabecular myocardium [13, 23].

A significant reduction in trabeculation (stage 2 above) is usually associated with ventricular compact zone deficiencies (hypoplastic wall), which commonly lead to embryonic heart failure and early embryonic lethality. In contrast, hypertrabeculation and lack of ventricular wall compaction (noncompaction) are closely related defects in cardiac embryogenesis associated with left ventricular noncompaction (LVNC). Although LVNC has been considered rare, recent surveys indicate that it is much more common than previously thought and a considerable number of patients survive into adulthood [45]. Indeed, LVNC can even be considered a third form of cardiomyopathy, in addition to dilated and hypertrophic cardiomyopathies [32, 36]. LVNC is clinically defined as a cardiomyopathy characterized by excessively thickened ventricular trabeculae and deep intertrabecular recesses based on echocardiogram diagnosis. It appears that LVNC is a genetically heterogeneous disorder [20, 46]. However, the etiology and pathogenesis of LVNC are largely unknown and reflect the lack of understanding of the underlying molecular and cellular mechanism(s) responsible for regulating ventricular trabeculation and compaction. Recently, several genetically engineered mouse models exhibiting various aspects of LVNC have been generated [19, 22, 39]. The FKBP12-deficient mouse line is one of them [41].

FKBP12 is a ubiquitously expressed 12-kDa cytoplasmic protein and belongs to the immunophilin family [5, 37]. FKBP12 has been shown to be associated with multiple intracellular protein complexes, including BMP/activin/TGF-β type I receptors [44] and Ca^{2+}-release channels, such as the inositol trisphosphate receptor (IP3R) and

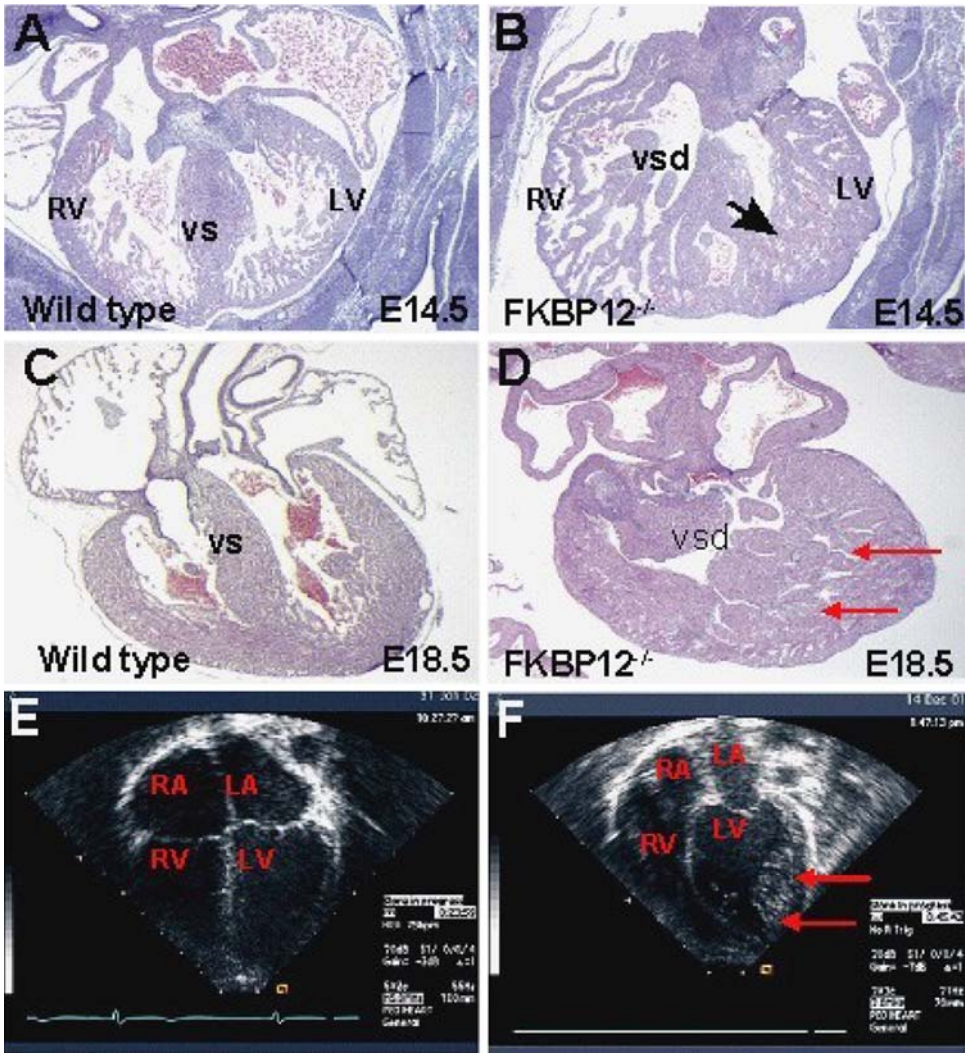

Fig. 1 Systemic FKBP12-null mice develop hypertrabeculated and noncompacted hearts, similar to NLVM in patients. **A–D** Cardiac histology of FKBP12-null hearts at E14.5 (**B**) and E18.5 (**D**) compared to that of wild-type littermates at E14.5 (**A**) and E18.5 (**C**). *Arrows* point to the characteristic excessive and thickened null ventricular trabeculae, which are accompanied by ventricular septal defects. **E**, **F** Echocardiographic images acquired from the four-chamber view of a 3-month-old patient with NLVM (**F**) and an age-matched unaffected patient (**E**). This image demonstrates excessive trabeculation in the posterior-lateral left ventricle wall (*red arrows*), which is very similar to that seen in FKBP12-deficient hearts. *LV* left ventricle, *RV* right ventricle, *LA* left atrium, *RA* right atrium, *vs* ventricular septum

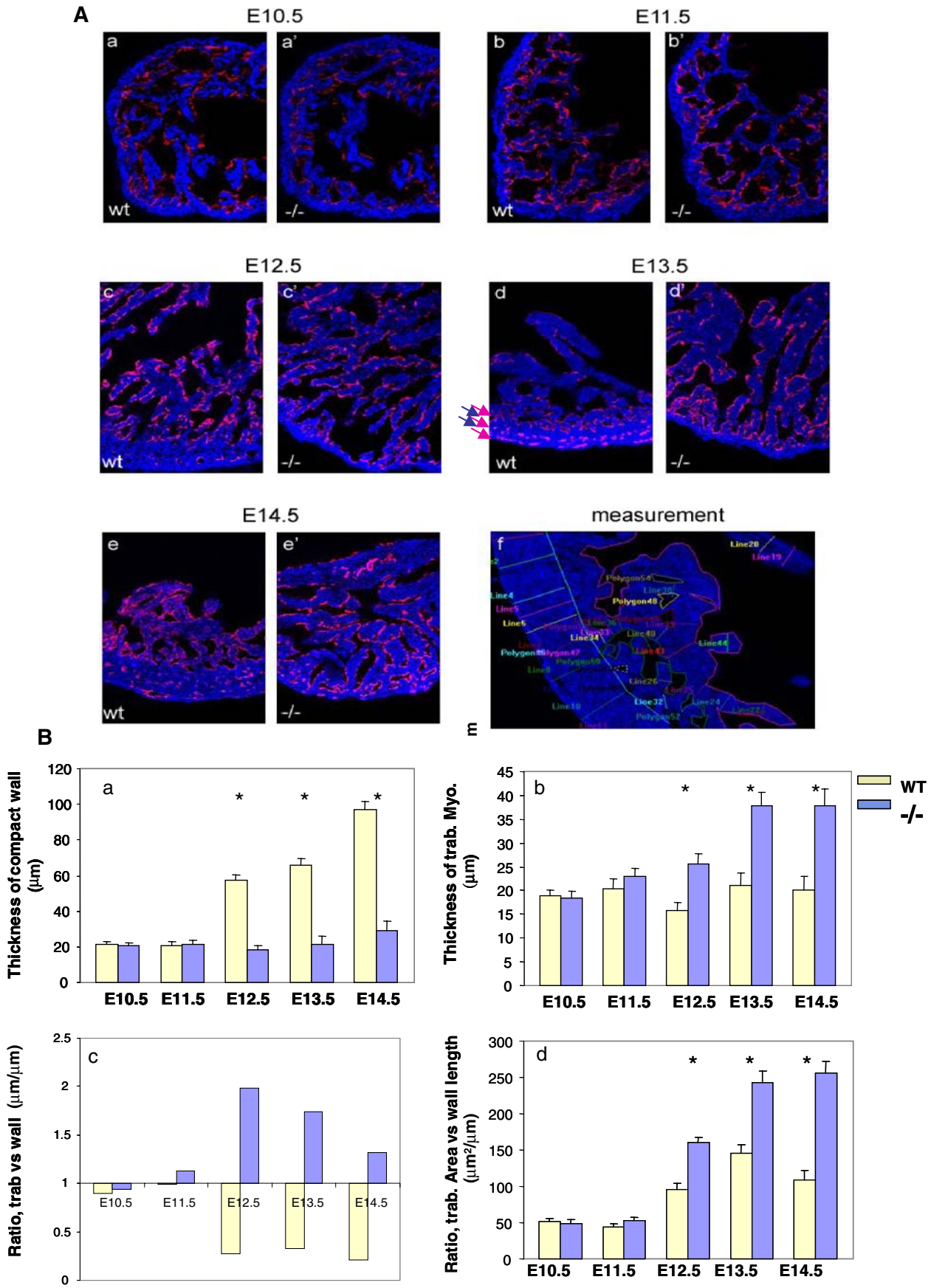
A
E10.5
E11.5
E12.5
E13.5
E14.5
measurement
wt
-/-
B
Thickness of compact wall (μm)
Thickness of trab. Myo. (μm)
Ratio, trab vs wall (μm/μm)
Ratio, trab. Area vs wall length (μm²/μm)
WT
-/-
E10.5
E11.5
E12.5
E13.5
E14.5

◀ **Fig. 2** Confocal image analysis of trabecular and compact myocardium. **A** Dual florescence merged images acquired from a confocal microscope. All images are from single-laser layer scanning (unstacked). CD31-positive (*red*) cells represent endocardium, while MF20 (*blue*) cells are myocardium. Cardiac trabeculation and compaction can be visually and quantitatively compared via this imaging analysis. (f) An example of measurement for the quantitative comparison. In addition, these images demonstrate that the endocardial endothelial cells form a thin endothelial layer extending up and around each trabecular sheet in both the wild-type and the FKBP12-null heart. This suggests that physical contact between endocardium and myocardium is normal in the FKBP12-null heart, whereas intercellular molecular signaling is likely disrupted. **B** Comparison of thickness of the wall (a) and the trabecular sheet (b), ratio of the thickness between the trabecular sheet and the compact wall (c), and ratio of overall trabecular area and length of the compact wall (d). * $p < 0.01$. (Original magnifications: ×200)

ryanodine receptor (RyR) [7, 8, 18, 43]. FKBP12-deficient mice die between embryonic day 14.5 (E14.5) and birth due to severe cardiac defects including a characteristic increase in the number and thickness of ventricular trabeculae, deep intertrabecular recesses, a lack of compaction, a thin ventricular wall, and a prominent ventricular septal defect (VSD) (Fig. 1) [41]. These cardiac defects are typical for LVNC. Therefore, the FKBP12-deficient mouse is a valuable model for studying the underlying mechanisms regulating ventricular trabeculation, compaction, and LVNC.

Previous studies on the morphogenetic process of ventricular trabeculation and compaction have so far relied heavily on histological descriptions, based on either light or

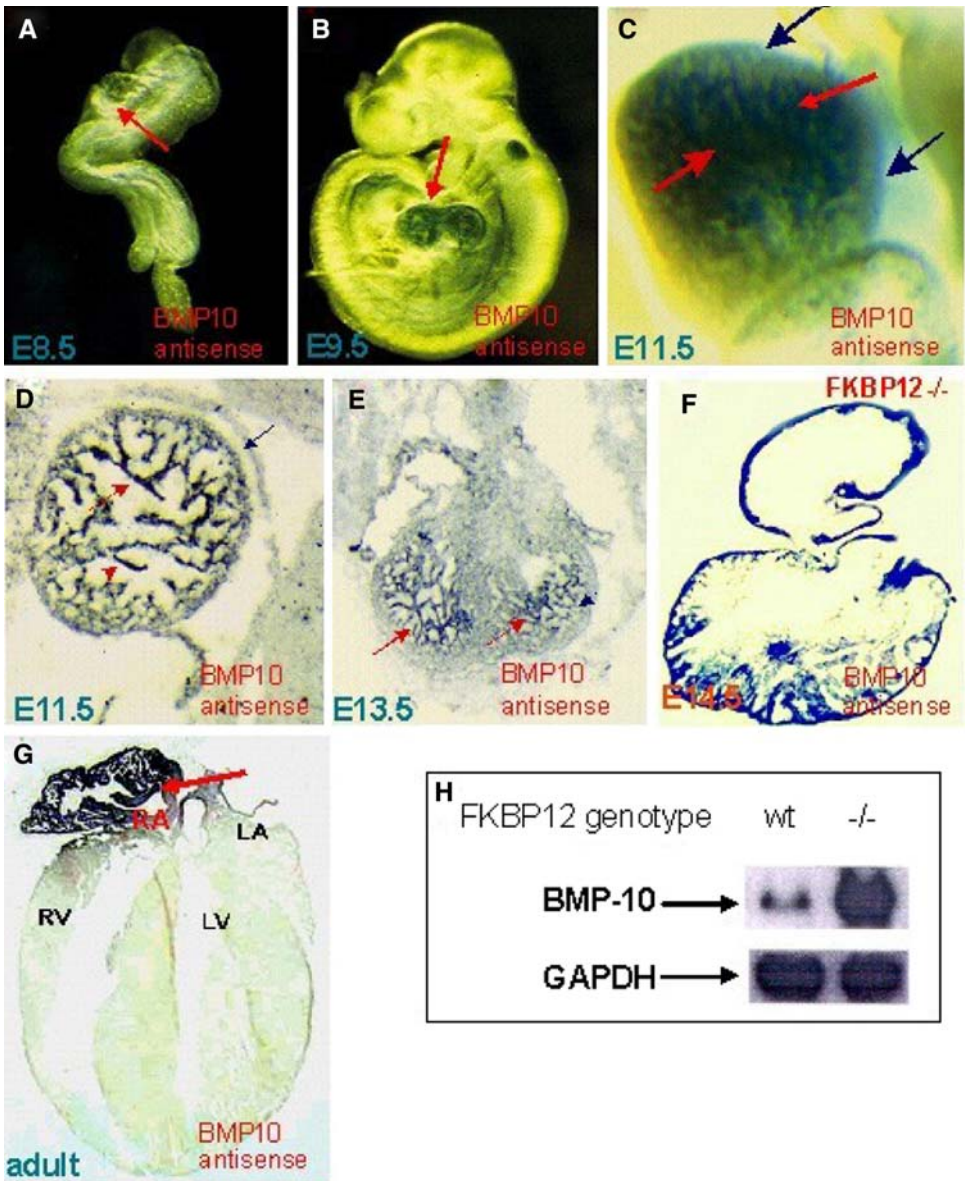

Fig. 3 Bmp10 expression is present only in the trabecular myocardium in mouse embryonic heart, whereas it is restricted to the right atrium in adult hearts. (**A–C**) Whole-mount and section (**D–G**) in situ analysis. Northern analysis revealed that Bmp10 expression is significantly overexpressed in FKBP12-null hearts compared to wild-type littermates (**H**)

scanning electron microscopic analyses [1, 2, 12, 27]. These conventional approaches are less reliable for analyzing and documenting cardiac defects in trabeculation and/or compaction in mutant mice because of difficulties in quantification. Inconsistencies using these tools have led to confusion in describing hypertrabeculation and noncompaction phenotypes. To systematically quantify and compare the dynamic processes of trabecular myocardial formation and compaction, we developed a dual-florescence imaging technique that is capable of quantifying the thickness of trabecular ridges and sheets, the overall thickness of the compact wall, and the ratio of trabecular myocardium to compact wall thickness. This methodology is based on confocal imaging of hearts immunostained with florescence-labeled anti-CD31 (PCAM, labeled with Alexa Fluor 488) and MF-20 (myosin heavy chain, labeled with Alexa Fluor 647) antibodies. Anti-CD31 immune reactivity highlights endothelial cells, including the endocardium lining the trabecular myocardium. MF-20 immune reactivity labels the myocardium. These immunostained hearts are serially cryosectioned (25 μm) in a four-chamber orientation. Sections with a similar orientation plane are used to generate a series of consecutive laser scanned images (Z series) that can be obtained by imaging serial confocal planes. This imaging system allows precise visualization of the architecture of the developing ventricular wall and the overall distribution and orientation of myocardial and endocardial cells, and distinguishes endothelial cells from myocardial cells for measurement of the thickness of trabecular ridges and sheets and of the compact wall. In addition, these digitized serial images can be further processed for three-dimensional reconstruction using Voxx software (Volume Rendering Program for 3D Microscopy) [11]. Most significantly, this quantitative imaging analysis methodology is capable of unbiased statistical testing and is able to unambiguously identify even subtle defects.

Figure 2 illustrates the use of this approach to analyze abnormal ventricular trabeculation and compaction in FKBP12-deficient hearts at E10.5 to E14.5. These images show that each trabecular myocardial sheet is wrapped with a thin endothelial cell layer. Remarkably, in addition to the dynamic process of trabecular growth, these images demonstrate for the first time the dramatic "layer-by-layer" process of normal ventricular compaction (arrows in Figs. 2a–d: red arrows indicate layers having a significant amount of newly formed capillaries, highlighted by the CD31-positive endocardium endothelium; blue arrows indicate layers having much less endocardium endothelium). In the FKBP12 mutant heart, this compaction process is defective. By tracing the trabeculae and compact walls, we are able to calculate the average thickness and overall areas of the trabecular myocardium and compact myocardium (Fig. 2b). Significant differences in cardiac trabeculation and compaction between wild-type and FKBP12-deficient heart can be seen as early as E11.5. Interestingly, as development proceeds, the ratio of trabecular myocardium thickness to compact wall thickness is reversed in FKBP12-deficient hearts compared to wild-type hearts. This analysis allows us to confirm that FKBP12-deficient mice are abnormal in the processes of both trabeculation and compaction.

Importantly, Bmp10 was dramatically up-regulated in FKBP12-null hearts, which was initially discovered during our gene profiling analysis and later further confirmed via Northern blot, RT-PCR, and in situ hybridization. Bmp10 is a peptide growth factor that belongs to the TGF-β superfamily [9, 29]. The spatial and temporal expression pattern of Bmp10 in mouse embryogenesis was assessed using whole-mount and section in situ hybridization (Fig. 3). During cardiac development, Bmp10 is expressed transiently in the

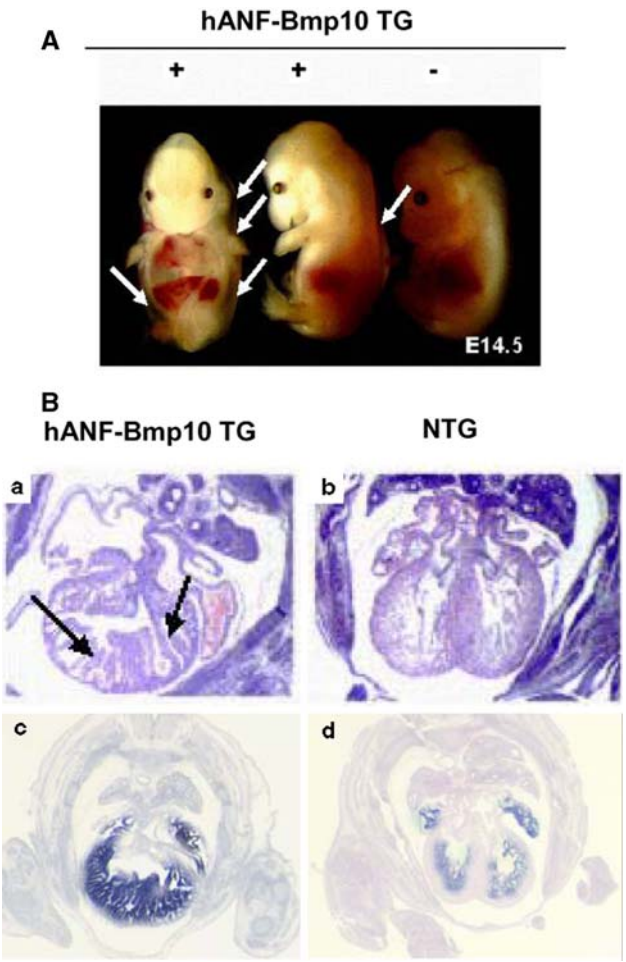

Fig. 4 Transgenic overexpression of Bmp10 in developing heart leads to excessive trabeculation and severe heart failure. **A** Gross morphology of hANF-BMP10 embryos. *White arrows* indicate body wall edema. **B** Cardiac histology (a, b) and BMP10 in situ hybridization confirm BMP10 expression in transgenic heart (c, d). *Black arrows* point to the abnormal trabeculae

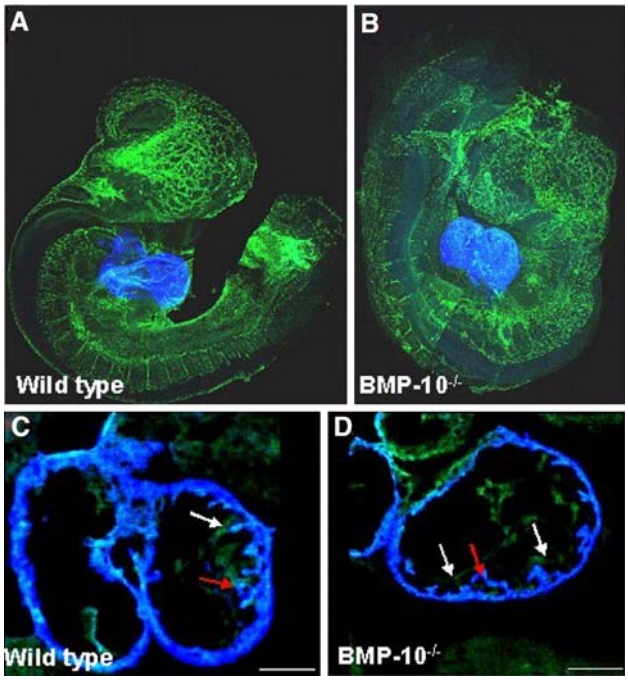

Fig. 5 Whole-mount immunostaining and confocal analysis of control (**A**, **C**) and Bmp10-deficient (**B**, **D**) embryos at E9.25. The Bmp10-deficient heart displays a much thinner wall. However, the primitive trabecular ridges are formed and the endocardium is in normal proximity to the myocardium. *Red arrows* trabecular ridge; *white arrows* endocardium

ventricular trabecular myocardium from E9.0 to E13.5, a critical time span when cardiac development shifts from patterning to growth and chamber maturation. By E16.5–E18.5, Bmp10 is detectable only in atria, and then only in right atria in postnatal hearts. Interestingly, the up-regulation of Bmp10 expression in myocardium is associated with another hypertrabeculation mouse model, Nkx2.5-myocardial-specific knockout mice [30], suggesting that Bmp10 is a key morphogenetic growth factor involved in the regulation of cardiac trabeculation and/or compaction.

To determine whether up-regulated Bmp10 expression would directly impact trabeculation and/or compaction in the developing myocardium, we used the human atrial natriuretic factor (hANF) promoter to drive exogeneous Bmp10 expression in mouse embryonic hearts. No viable hANF-Bmp10 mice were found. In situ hybridization demonstrated significant up-regulation of Bmp10 in hANF-Bmp10 hearts. Histological examination showed that the eight highest-expressing hANF-Bmp10-positive hearts all exhibited hypertrabeculation and noncompaction (Fig. 4) [30]. These data demonstrate that overexpression of Bmp10 alone is sufficient to cause cardiac hypertrabeculation and noncompaction as seen in FKBP12-deficient hearts.

Bmp10-deficient mice were generated to analyze its role in ventricular development [9]. Bmp10-deficient embryos appear to be normal at E8.5–E9.0, suggesting that Bmp10 is not required for initial cardiac patterning and cardiac looping. At E9.0–E9.5, cardiogenesis appears to be arrested and null embryos die in utero at E10.5 due to poorly developed hearts. These mutant embryos display cardiac dysgenesis, with profound hypoplastic ventricular walls and an absence of ventricular trabeculae. Using immunohistochemical staining and confocal microscopy, we analyzed the formation of the primitive trabecular ridge and the endocardial structure in Bmp10-deficient hearts. As shown in Fig. 5, using Flk-1 (endothelial receptor for VEGF) as an endocardial marker (green) and MF20 as a myocardial marker (blue), we have observed that the developing endocardium is in normal proximity to the ventricular wall and the primitive trabecular ridges are actually formed in mutant hearts. This finding indicates

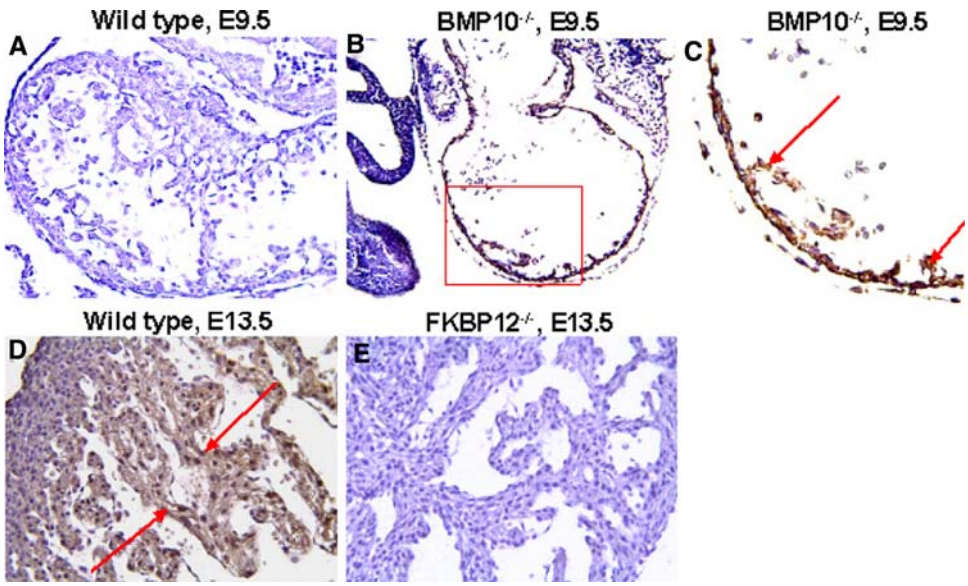

Fig. 6 Distribution and expression of $p57^{kip2}$ in BMP10-deficient and FKBP12-deficient hearts using immunohistochemistry staining. At E9.5, $p57^{kip2}$ expression was undetectable in wild-type heart (**A**) but was ectopically present in the BMP10-deficient heart (**B**, **C**) under identical staining conditions. Expression of $p57^{kip2}$ was abundant in E13.5 ventricular trabecular myocardium of wild-type heart (**D**) but was significantly down-regulated in E13.5 FKBP12-deficient trabecular myocardium (**E**). *Arrows* indicate areas of positive staining

that Bmp10 is not critical to the initiation of cardiac trabeculation but is essential for subsequent growth. Consistent with this observation, there was a marked reduction in proliferation (using ^{3}H-thymidine to monitor DNA synthesis) in Bmp10-deficient cardiomyocytes [9].

p57^{kip2} is a critical negative cell cycle regulator [4]. Interestingly, p57^{kip2} expression is first detectable in the developing mouse heart at E10.5 and is restricted to the ventricular trabecular myocardium [21]. Therefore, p57^{kip2} is considered a key negative regulator involved in cardiac cell cycle exit within the developing ventricular trabeculae during chamber maturation. Immunohistochemistry staining reveals that p57^{kip2} is up-regulated and ectopically expressed throughout the ventricular wall in Bmp10-null hearts at E9.5 compared to wild-type littermate controls (Fig. 6). Significantly, FKBP12-deficient hearts (E13.5), which show elevated Bmp10 expression and overproduction of trabeculae, exhibit significantly lower p57^{kip2} levels in trabecular myocardium compared to control littermates (Fig. 6). Using the ^{3}H-thymidine incorporation assay, there is significant enhancement of proliferative activity in FKBP12-deficient trabecular myocardium, while there is no obvious difference in the compact myocardial wall compared to normal controls (Fig. 7). Consistent with the increase in proliferative activity of trabecular myocardium, the process of cellular differentiation and maturation of cardiomyocytes in trabecular myocardium is also defective in FKBP12-deficient hearts. In normal myocardium at E9.5, trabecular cells show a more advanced state of cellular differentiation, as reflected by a more mature and organized sarcomere with a higher density of Z-lines/bodies, while cardiomyocytes in the compact wall have significantly fewer Z-lines/bodies [14, 34]. By E13.5, both the trabecular and the compact myocardium will have matured normally and have organized sarcomeres. In FKBP12-deficient embryonic hearts (E13.5), the organization of sarcomeres in trabecular cardiomyocytes is not yet established compared to normal littermate controls (Fig. 8). This suggests that the normal balance of proliferation and differentiation is altered in FKBP12-deficient myocardium (i.e., higher proliferative activity and a lower differentiation state).

Taken together, these data indicate that hypertrabeculation is likely the result of altered regulation in cell proliferation, differentiation, and maturation during ventricular wall formation. In addition, Bmp10 is an important regulator for this spatiotemporally controlled cell cycle activity in cardiac trabeculation via its direct or indirect regulation of p57^{kip2}. However, it is not entirely clear whether noncompaction is a result of hypertrabeculation or an independent pathological event. Our recent study analyzing the Smad7-deficient mouse heart indicates that noncompaction of myocardium can occur without an overall increase in cell proliferative activity in trabecular myocardium [10],

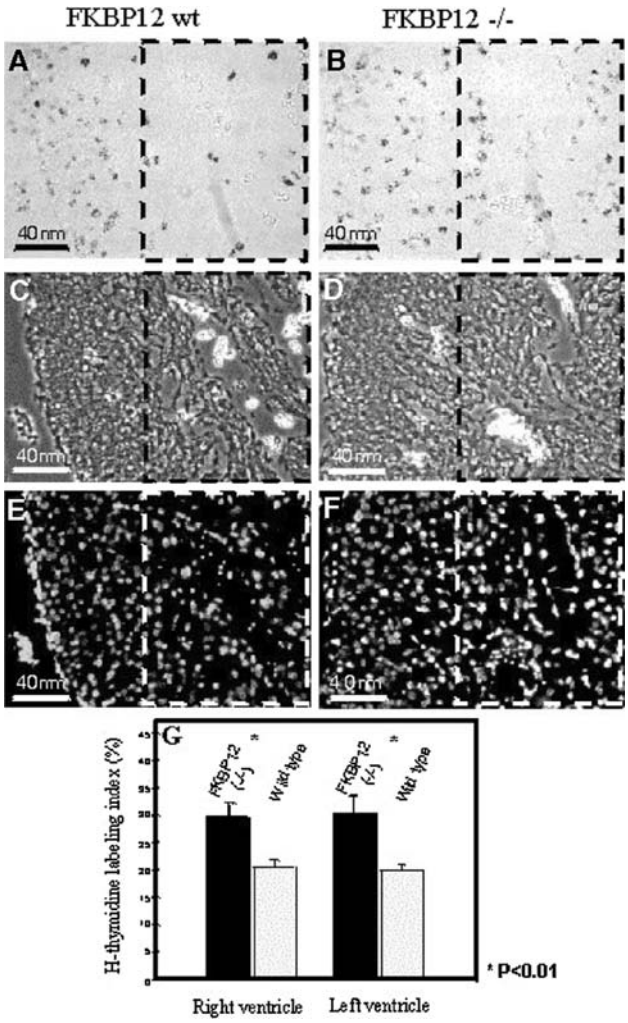

Fig. 7 Comparison of ^{3}H-thymidine labeling index of FKBP12-deficient heart versus littermate control heart (E14.5). *Boxed* areas in **A**–**F** highlight the ventricular trabeculae. FKBP12-deficient heart has a significantly higher labeling index, suggesting higher proliferation activity in the FKBP12-deficient heart. **A**, **B** ^{3}H-Thymidine-labeled heart; **C**, **D** phase contrast of the same ventricular region shown in **A** and **B**; **E**, **F** Hoechst staining to show the nucleus of the same region as in **A** and **B**; **G** statistical comparison of the cardiac ^{3}H-thymidine labeling index in the trabecular myocardium. There is no significant difference in the compact wall

suggesting that the failure of myocardial compaction is likely an independent pathological event. Interestingly, Smad7 is an important negative regulator for the BMP/TGF-β-mediated signaling pathway [15, 40]. Ablation of Smad7 leads to elevated levels of activated Smad1/5/8, but not Smad2/3, in developing endocardial endothelial cells [10], suggesting that the cardiac endothelium plays an important role in ventricular myocardial compaction, likely via BMP-mediated signaling. Future studies will address the molecular mechanism by which FKBP12 regulates the expression of Bmp10. It is also important to determine the spatial and temporal regulation of FKBP12 activity and

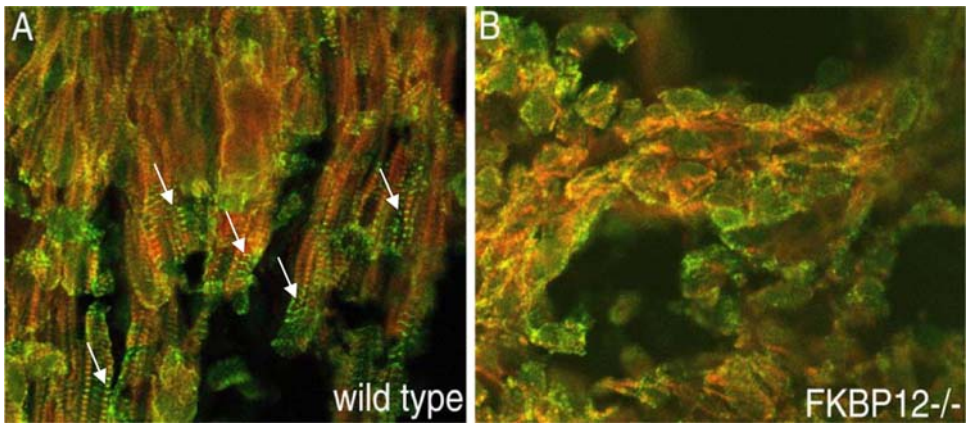

Fig. 8 Comparison of myofibrillogenesis in FKBP12-deficient and wild-type ventricular trabecular myocardium (E13.5). Frozen cardiac sections were stained with anti-α-actinin monoclonal antibody for Z-line (FITC labeled) and counter-stained with anti-F-actin (rhodamine labeled). Confocal images were acquired using a Zeiss LSM 510 laser microscope. **A** Wild-type trabecular myocardium contains well-organized sarcomeres (*white arrows*). **B** There are no mature sarcomeres in FKBP12-deficient trabecular myocardium. In addition, instead of an elongated cellular morphology in the wild type, most FKBP12-deficient cardiomyocytes appear to be rounded, an indication of underdifferentiation

BMP10 expression in LVNC patients. The knowledge gained from these studies will to elucidate the etiology of LVNC in patients.

Acknowledgment This study was supported in part by National Institutes of Health Grants HL81092 (W.S.), HL70259 (W.S.), and HL85098 (W.S., M.P.).

References

1. Anderson RH, Webb S et al (2003) Development of the heart: (2) Septation of the atriums and ventricles. Heart 89(8):949–958
2. Anderson RH, Webb S et al (2003) Development of the heart: (3) Formation of the ventricular outflow tracts, arterial valves, and intrapericardial arterial trunks. Heart 89(9):1110–1118
3. Bartman T, Hove J (2005) Mechanics and function in heart morphogenesis. Dev Dynam 233(2):373–381
4. Besson A, Dowdy SF et al (2008) CDK inhibitors: cell cycle regulators and beyond. Dev Cell 14(2):159–169
5. Bierer BE, Mattila PS et al (1990) Two distinct signal transmission pathways in T lymphocytes are inhibited by complexes formed between an immunophilin and either FK506 or rapamycin. Proc Natl Acad Sci USA 87(23):9231–9235
6. Brutsaer DL, Andries LJ (1992) The endocardial endothelium. Am J Physiol 263(4; Pt 2):H985–H1002
7. Cameron AM, Nucifora FC Jr et al (1997) FKBP12 binds the inositol 1,4,5-trisphosphate receptor at leucine-proline (1400–1401) and anchors calcineurin to this FK506-like domain. J Biol Chem 272(44):27582–27588
8. Cameron AM, Steiner JP et al (1995) Calcineurin associated with the inositol 1,4,5-trisphosphate receptor-FKBP12 complex modulates Ca2+ flux. Cell 83(3):463–472
9. Chen H, Shi S et al (2004) BMP10 is essential for maintaining cardiac growth during murine cardiogenesis. Development 131(9): 2219–2231
10. Chen Q, Chen H et al (2009) Smad7 is required for the development and function of heart. J Biol Chem 284(1):292–300
11. Clendenon JL, Phillips CL et al (2002) Voxx: a PC-based, near real-time volume rendering system for biological microscopy. Am J Physiol Cell Physiol 282(1):C213–C218
12. Cook AC, Yates RW et al (2004) Normal and abnormal fetal cardiac anatomy. Prenat Diagn 24(13):1032–1048
13. Gourdie RG, Kubalak S et al (1999) Conducting the embryonic heart: orchestrating development of specialized cardiac tissues. Trends Cardiovasc Med 9(1–2):18–26
14. Hagopian M, Spiro D (1970) Derivation of the Z line in the embryonic chick heart. J Cell Biol 44(3):683–687
15. Heldin CH, Miyazono K et al (1997) TGF-beta signalling from cell membrane to nucleus through SMAD proteins. Nature 390(6659):465–471
16. Icardo JM (1988) Heart anatomy and developmental biology. Experientia 44(11–12):910–919
17. Icardo JM, Fernandez-Teran A (1987) Morphologic study of ventricular trabeculation in the embryonic chick heart. Acta Anat (Basel) 130(3):264–274
18. Jayaraman T, Brillantes AM et al (1992) FK506 binding protein associated with the calcium release channel (ryanodine receptor). J Biol Chem 267(14):9474–9477
19. King T, Bland Y et al (2002) Expression of Peg1 (Mest) in the developing mouse heart: involvement in trabeculation. Dev Dynam 225(2):212–215
20. Klaassen S, Probst S et al (2008) Mutations in sarcomere protein genes in left ventricular noncompaction. Circulation 117(22): 2893–2901
21. Kochilas LK, Li J et al (1999) p57Kip2 expression is enhanced during mid-cardiac murine development and is restricted to trabecular myocardium. Pediatr Res 45(5; Pt 1):635–642
22. Lee Y, Song AJ et al (2000) Jumonji, a nuclear protein that is necessary for normal heart development. Circ Res 86(9):932–938
23. Meilhac SM, Kelly RG et al (2003) A retrospective clonal analysis of the myocardium reveals two phases of clonal growth in the developing mouse heart. Development 130(16):3877–3889
24. Mikawa T, Borisov A et al (1992) Clonal analysis of cardiac morphogenesis in the chicken embryo using a replication-defective retrovirus: I. Formation of the ventricular myocardium. Dev Dynam 193(1):11–23

25. Mikawa T, Cohen-Gould L et al (1992) Clonal analysis of cardiac morphogenesis in the chicken embryo using a replication-defective retrovirus: III. Polyclonal origin of adjacent ventricular myocytes. Dev Dynam 195(2):133–141
26. Mikawa T, Gourdie RG et al (2002) Induction and patterning of the Purkinje fibre network. Novartis Found Symp 250:142–153; discussion 153–156
27. Moorman A, Webb S et al (2003) Development of the heart: (1) Formation of the cardiac chambers and arterial trunks. Heart 89(7):806–814
28. Moorman AF, Christoffels VM et al (2007) The heart-forming fields: one or multiple? Philos Trans R Soc Lond Ser B Biol Sci 362(1484):1257–1265
29. Neuhaus H, Rosen V et al (1999) Heart specific expression of mouse BMP-10, a novel member of the TGF-beta superfamily. Mech Dev 80(2):181–184
30. Pashmforoush M, Lu JT et al (2004) Nkx2-5 pathways and congenital heart disease; loss of ventricular myocyte lineage specification leads to progressive cardiomyopathy and complete heart block. Cell 117(3):373–386
31. Pasumarthi KB, Field LJ (2002) Cardiomyocyte cell cycle regulation. Circ Res 90(10):1044–1054
32. Pignatelli RH, McMahon CJ et al (2003) Clinical characterization of left ventricular noncompaction in children: a relatively common form of cardiomyopathy. Circulation 108(21):2672–2678
33. Risebro CA, Riley PR (2006) Formation of the ventricles. Sci World J 6:1862–1880
34. Ronna KC (1977) Myogenesis and contraction in the early embryonic heart of the rainbow trout. An electron microscopic study. Cell Tissue Res 180(1):123–132
35. Rumyantsev PP, Krylova MI (1990) Ultrastructure of myofibers and cells synthesizing DNA in the developing and regenerating lymph-heart muscles. Int Rev Cytol 120:1–52
36. Sandhu R, Finkelhor RS et al (2008) Prevalence and characteristics of left ventricular noncompaction in a community hospital cohort of patients with systolic dysfunction. Echocardiography 25(1):8–12
37. Schreiber SL, Crabtree GR (1995) Immunophilins, ligands, and the control of signal transduction. Harvey Lect 91:99–114
38. Sedmera D, Pexieder T et al (2000) Developmental patterning of the myocardium. Anat Rec 258(4):319–337
39. Shi W, Chen H et al (2003) TACE is required for fetal murine cardiac development and modeling. Dev Biol 261(2):371–380
40. Shi Y, Massague J (2003) Mechanisms of TGF-beta signaling from cell membrane to the nucleus. Cell 113(6):685–700
41. Shou W, Aghdasi B et al (1998) Cardiac defects and altered ryanodine receptor function in mice lacking FKBP12. Nature 391(6666):489–492
42. Taber LA (1998) Mechanical aspects of cardiac development. Prog Biophys Mol Biol 69(2–3):237–255
43. Timerman AP, Ogunbumni E et al (1993) The calcium release channel of sarcoplasmic reticulum is modulated by FK-506-binding protein. Dissociation and reconstitution of FKBP-12 to the calcium release channel of skeletal muscle sarcoplasmic reticulum. J Biol Chem 268(31):22992–22999
44. Wang T, Li BY et al (1996) The immunophilin FKBP12 functions as a common inhibitor of the TGF beta family type I receptors. Cell 86(3):435–444
45. Weiford BC, Subbarao VD et al (2004) Noncompaction of the ventricular myocardium. Circulation 109(24):2965–2971
46. Xing Y, Ichida F et al (2006) Genetic analysis in patients with left ventricular noncompaction and evidence for genetic heterogeneity. Mol Genet Metab 88(1):71–77